ELSEVIER

J. Non-Newtonian Fluid Mech. 116 (2004) 183–204

Journal of Non-Newtonian Fluid Mechanics

www.elsevier.com/locate/jnnfm

Scaling behavior of kinetic orientational distributions for dilute nematic polymers in weak shear

M. Gregory Forest [a], Ruhai Zhou [a], Qi Wang [b]

[a] *Department of Mathematics, University of North Carolina at Chapel Hill, Chapel Hill, NC 27599, USA*
[b] *Department of Mathematical Sciences, Florida State University, Tallahassee, FL 32306, USA*

Received 24 April 2003; received in revised form 18 July 2003

Abstract

Analytical descriptions of shear-aligned nematic monodomains have a long history across continuum, mesoscopic and mean-field kinetic models. Their value lies in the prediction of explicit scaling properties of the orientational distribution and of normal and shear stresses, with respect to molecular and flow parameters. At the coarsest scale of continuum Leslie–Ericksen theory [Arch. Rational Mech. Anal. 4 (1960) 231; Arch. Rational Mech. Anal. 28 (1968) 265], an explicit macroscopic alignment angle formula always exists in terms of bulk Miesowicz viscosities; the theory applies only to nematic (highly concentrated) liquids with low molecular weight and in the weak flow limit [Phys. Soc. Jpn. 52 (1983) 3486; Phys. Soc. Jpn. 53 (1984) 1031; J. Chem. Phys. 116 (2002) 9120; A hydrodynamic theory for solutions of non-homogeneous nematic liquid crystalline polymers with density variations, in: Proceedings of ASME International Mechanical Engineering Congress, IMECE2002-32189, N.O., LA, 17-22 November 2002]. At mesoscales, orientation tensor models [J. Chem. Phys. 103 (1995) 3108; The Physics of Liquid Crystals, Oxford University Press, Oxford, 1993; Thermodynamics of Flowing Systems with Internal Microstructure, Oxford Science Publications, Oxford, 1994; J. Chem. Phys. 103 (1995) 807; The Structure and Rheology of Complex Fluids, Oxford University Press, Oxford, 1998] apply at all concentrations and shear rates; explicit "Leslie angle" formulas exist only in the weak shear limit [Macromolecules 23 (1990) 4446; J. Rheol. 37 (1993) 413; J. Rheol. 37 (1993) 289; J. Rheol. 41 (1997) 943; Phys. A 267 (1999) 294; J. Non-Newtonian Fluid Mech. 90 (2000) 283; Rheol. Acta 42 (2003) 20; J. Rheol. 47 (2003) 105], inheriting hysteresis in alignment properties from the quiescent isotropic–nematic transition. Since the fundamental results of Onsager [Ann. N.Y. Acad. Sci. 51 (1949) 627] for quiescent nematic equilibria, exact probability distribution functions (PDFs) of kinetic theory have proven elusive for flow-driven nematic states. In their stead, flow-aligned and unsteady PDF formulas, elegant though implicit, have been derived by Kuzuu–Doi [Phys. Soc. Jpn. 52 (1983) 3486; Phys. Soc. Jpn. 53 (1984) 1031] and Semenov [Sov. Phys. JETP 66 (1983) 321] by weak flow asymptotic analysis, and by Marrucci and Maffettone [Macromolecules 22 (1989) 4076] by restriction to two dimensions. A simpler problem concerns the dilute concentration regime where the quiescent equilibrium is isotropic, non-degenerate, and stable, which is the focus of this paper. Using weak-flow asymptotics, we explicitly construct, and establish stability of, stationary, shear-perturbed PDFs for dilute concentrations; our formulas prove unsteady tumbling of perturbed isotropic states cannot occur. Exact scaling properties are predicted, including explicit Leslie alignment angle and degree-of-alignment (birefringence) formulas, as well as normal and shear stresses, in terms of molecular parameters and normalized shear rate for dilute nematic polymers. Our formulas apply except in a neighborhood of the isotropic instability transition, which See et al. [J. Chem. Phys. 92 (1990)

0377-0257/$ – see front matter © 2003 Elsevier B.V. All rights reserved.
doi:10.1016/j.jnnfm.2003.07.002

792] analyzed by a singular perturbation analysis. We then show how to bridge our method with that of See et al. [J. Chem. Phys. 92 (1990) 792], thereby completing the existence, construction, and stability of shear-perturbed isotropic equilibria for all concentrations. We verify the formulas both by numerical simulations and by comparison with mesoscopic model predictions [Rheol. Acta 42 (2003) 20; J. Rheol. 47 (2003) 105; J. Chem. Phys. 92 (1990) 792].
© 2003 Elsevier B.V. All rights reserved.

Keywords: Nematic polymers; Kinetic theory; Rheology; Shear flow

1. Introduction

A classical benchmark of continuum, mesoscopic, and molecular theory for nematic polymers is the ability to predict conditions under which monodomain flow-alignment occurs (cf. [24,25]), the resultant most probable direction of alignment (the "major director"), the relative focusing or spreading of the orientational distribution (the order parameters), and to parametrize these properties in terms of model parameters. As one passes down from coarser to finer scale models, the ability to do explicit analysis is compromised. Leslie–Ericksen (L–E) *continuum theory* [1,2] gives explicit in-plane alignment condition and Leslie angle formula, which depend only on Miesowicz viscosities, independent of shear rate, without information on the spread of the orientational distribution. These results apply only to strongly nematic, small-molecular-weight liquids (liquid crystals), so that continuum theory gives no information for dilute concentrations of nematic polymers; indeed, there is no concentration parameter in the theory.

Quiescent nematic polymers have multiple stable phases (isotropic in the dilute regime, nematic at high concentrations, with bistability in an overlap regime). When shear flow is imposed, steady alignment sometimes occurs, and it is a challenge of mesoscopic or kinetic theory to predict a most probable alignment angle in terms of model parameters, and to ascertain whether the distribution is steady or oscillatory. This analog of the Leslie alignment angle is known to vary with shear rate and concentration, and there is ample theoretical evidence for strong dependence on molecular aspect ratio at nematic concentrations [7,10,18,19]. *Mesoscopic models* describe shear-aligned steady states, but explicit formulas are only available in the weak shear limit [12–19]. In this limit, the authors derived the Leslie angle dependence upon molecular aspect ratio and concentration, whereas shear rate dependence requires higher order asymptotic analysis [19] or direct numerical simulation [18,19]. Furthermore, the Leslie angle of stable states varies abruptly for dilute versus concentrated nematics, as expected since the flow-aligned solution branches arise from two distinct quiescent states (the isotropic and the nematic).

In *kinetic theory*, exact expressions for the orientational probability distribution function in shear flow are not yet available, although several useful and illustrating approximations have been derived [3,4,6,7,9–11,21,23]. The utility of explicit formulas lies in their prediction of how molecular alignment features scale with properties of the nematic polymer and flow. The difficulty in gaining explicit formulas is not surprising, with very little analytical progress since the seminal paper of Onsager [20] and the above references. New insights, Constantin et al. [26], appear to be emerging. Marrucci and Maffettone [22] finessed the problem by restricting to two dimensions and made remarkable progress, especially in the explanation of negative normal stress differences. Numerical simulations [27–29] show that shear-perturbed nematic equilibria have significant high-order spherical harmonic amplitudes, and there is no natural known classical distribution that resolves the numerical results. Furthermore, all

nematic equilibria are orientationally degenerate [8,20,29,30], so their perturbed properties are inherently complex; the breakup and persistence of the orthogonal group of nematic equilibria has only succumbed to partial analysis in mesoscopic models [19].

By comparison, the isotropic branch is trivial (constant) for kinetic theory as well as mesoscopic theory, so one might expect to be able to carry out a weak-shear asymptotic analysis for this shear-deformed isotropic branch. Such an analysis is relevant experimentally only in the dilute regime below the "clearing transition", where quiescent nematic polymers are isotropic (except for a short interval of bi-stability). Imposed shear flows in the isotropic concentration range are known to induce weak birefringence (cf. [22]), with peaks in the orientational distribution focused in the shear plane, at the Leslie alignment angle, as predicted from essentially all mesoscopic models [18,19]. See et al. [23] developed a singular perturbation analysis in the weak flow limit, centered at the isotropic transition, in order to show that flow perturbations shift the instability of the isotropic state to *lower* concentrations.

Our goal in this paper is to establish analytical scaling properties of the perturbed isotropic branch directly from kinetic theory in the weak shear limit, and to give explicit formulas for the alignment angle, degrees of alignment, and normal and shear stresses, parametrized in terms of molecular parameters and normalized shear rate. Our analysis is complementary to See et al. [23], in that it applies everywhere *except* in a neighborhood of the isotropic transition. To complete the flow-perturbed analysis of isotropic equilibria for all concentrations, we show how to connect the regular expansion away from the isotropic transition to the singular expansion employed in [23]. We show, for example, that the isotropic instability corresponds to a *fifth-order degeneracy* in the marginal stability condition for the linearized Smoluchowski equation. This degeneracy (with a multiplicity five linearized eigenvalue) occurs for *all* concentrations, and we show the eigenfunctions are precisely the second-moment tensor basis. From this analytical structure, we show how the quiescent, highly degenerate, isotropic bifurcation point splits, separated by a gap with no persistent isotropic states, into a pair of saddle-nodes, or turning points. The See et al. [23] bifurcation curve is the "left" turning point, marking the onset of instability of the shear-perturbed isotropic branch at *lower* concentrations than the quiescent values. The right turning point marks the continuation of unstable isotropic equilibria in shear.

We employ the Doi kinetic theory, extended to include a finite aspect ratio of spheroidal molecules [5]; we then develop a weak-shear asymptotic expansion of the probability distribution function (f) by an extension of the seminal methods of Kuzuu and Doi [3,4] and See et al. [23]. At leading order, the quiescent equilibrium distribution functions consist of: the isotropic state ($f = 1/(4\pi)$) for all concentrations N (dimensionless), which is stable only for $0 < N < N_2 = 5$; and, a pair of nematic equilibria above a critical concentration $N_1 \approx 4.49$. For the quiescent nematic equilibria [20], weak shear asymptotic corrections are thus far inaccessible to our analysis. We are nonetheless motivated by the approximations predicted by Semenov [21], Stepanov [31], Archer and Larson [7] and Kroger and Sellers [10] for the shear-aligned nematic steady state, which provide an expression for the Leslie tumbling parameter, λ,

$$\lambda = a\frac{5P_2 + 16P_4 + 14}{35P_2}, \tag{1}$$

where $a = (r^2 - 1)/(r^2 + 1)$, r is the molecular aspect ratio, and P_2, P_4 are equilibrium values of the second and fourth moments of the PDF f, given in terms of Legendre polynomials. The Leslie alignment angle ϕ for flow-aligning nematics is then given by

$$\cos(2\phi) = \lambda^{-1}, \tag{2}$$

which takes the same form in mesoscopic tensor analysis [12–19]. (As we shall confirm below, the kinetic theory analog of the Leslie tumbling parameter for the isotropic branch in weak shear is a "flow-aligning parameter", since dilute concentrations of nematic polymers do not tumble at weak to moderate shear rates.) According to (1), flow-alignment occurs only when $|\lambda| \geq 1$. The moments $P_{2,4}$ are concentration-dependent, and can be computed numerically as functions of N; therefore if $|a| = 1$, the Leslie angle and unsteady transition can be tabulated versus N. The molecular geometry parameter a lies between $a = -1$ for infinitely thin discs, $a = 0$ for spherical molecules, and $a = +1$ for infinitely thin rods; $|a|$ decreases monotonically from 1 to 0 from extreme aspect ratios to the spherical molecule limit. From (1), as noted by Archer and Larson, the effect of reducing the aspect ratio, e.g. from $a = 1$ to $a = 0.8$ ($r = 3$), can be quite significant. If the infinite aspect ratio nematic liquid is tumbling, lowering aspect ratio will only enhance tumbling, i.e., shorten the period. However, a flow-aligned infinite aspect ratio liquid is transformed by lowering aspect ratio to *either* reduce the Leslie angle downward (toward the flow axis) *or* cause a tumbling transition. This effect due to aspect ratio has been explored in [18] for a variety of mesoscopic closure approximations to the Doi theory, and in [19] from an analytical tensor method which yields precise curves $N(a)$ along which the steady-unsteady transition occurs. These phenomena are specific to the nematic state in weak shear, and rigorous analysis only exists from mesoscopic tensor models in the weak shear limit, together with the elegant kinetic PDF treatments of Semenov [21] and Marrucci and Maffettone [22].

By focusing on the weak-shear continuation of the isotropic state, at low and high concentrations, we will derive explicit kinetic theory formulas of the form (1). Indeed, we will construct the stationary PDF, then its moments, and all average orientation properties become explicit. We thereby affirm the validity of such exact kinetic theory expressions.

Our regular asymptotic analysis is shown to become disordered where the isotropic state destabilizes, precisely the focus of the See et al. [23] analysis. Indeed, their formulas are sufficient to give the alignment properties of states *on the bifurcation branch*, although they did not choose to extract this information in their paper. To close the book on the deformation of isotropic equilibria in weak flows for all concentrations, we show how to deduce the See et al. [23] expansion in powers of $Pe^{1/2}$, where Pe is the normalized shear rate. This scaling is equivalent to showing the quiescent bifurcation point of the isotropic instability splits into two turning points (two saddle-node bifurcations), separated by a gap in concentrations of $O(Pe^{1/2})$ around $N = 5$. Inside the gap the quiescent isotropic stationary distributions do not persist in weak shear. The right turning point and construction of the PDF for $N > 5 + O(Pe^{1/2})$ are given, corresponding to unstable, nearly isotropic persistent states, not believed to be physically realizable. We note, as a curiosity, that nearly isotropic monodomains of concentrated nematic polymers are transiently observed in numerical simulations of structure formation in shear cells [32,33], associated with local defects that mediate neighboring incompatible orientational patterns, as anticipated by Marrucci and Greco [30].

2. Kinetic theory for LCPs of spheroidal molecules

Let $f(\boldsymbol{m}, t)$ be the orientational probability distribution function for molecules with axis of symmetry $\boldsymbol{m}$ on the unit sphere S^2 in a linear flow field

$$\boldsymbol{v} = (\boldsymbol{\Omega} + \boldsymbol{D}) \cdot \boldsymbol{x}, \tag{3}$$

where $\boldsymbol{\Omega}$ and $\boldsymbol{D}$ are vorticity and rate-of-strain tensors, respectively. The Smoluchowski (kinetic) equation for $f(\boldsymbol{m}, t)$ is given by [5]

$$\frac{Df}{Dt} = \mathcal{R}\cdot[D_{\mathrm{r}}(\boldsymbol{m})(\mathcal{R}f + \frac{1}{kT} f\mathcal{R}V)] - \mathcal{R}\cdot[\boldsymbol{m}\times\dot{\boldsymbol{m}}f],$$
$$\dot{\boldsymbol{m}} = \boldsymbol{\Omega}\cdot\boldsymbol{m} + a[\boldsymbol{D}\cdot\boldsymbol{m} - \boldsymbol{D}:mmm], \tag{4}$$

where $D_{\mathrm{r}}(\boldsymbol{m})$ is the rotary diffusivity which we hold constant, $D_{\mathrm{r}}(\boldsymbol{m}) = D_{\mathrm{r}}^0$, to make connection with [28,34]; k is the Boltzmann constant; T is the absolute temperature; $\mathcal{R} = \boldsymbol{m}\times(\partial/\partial\boldsymbol{m})$ is the rotational gradient operator; and $(\mathrm{D}/\mathrm{D}t)(\cdot)$ denotes the material derivative $(\partial/\partial t)(\cdot) + \boldsymbol{v}\cdot\nabla(\cdot)$. In (4), the second moment of $\boldsymbol{m}$,

$$\boldsymbol{M} = \langle mm\rangle = \int_{\|\boldsymbol{m}\|=1} \boldsymbol{m}\boldsymbol{m}\, f(\boldsymbol{m}, t)\,\mathrm{d}\boldsymbol{m}, \tag{5}$$

enters through the mean-field Maier–Saupe excluded-volume potential V,

$$V = -\tfrac{3}{2}NkT\boldsymbol{m}\boldsymbol{m} : \boldsymbol{M}. \tag{6}$$

The mesoscopic orientation tensor $\boldsymbol{Q}$ is the traceless form of $\boldsymbol{M}$, whose eigenvalues and eigenvectors provide the mesoscopic order parameters and directors:

$$\boldsymbol{Q} = \boldsymbol{M} - \tfrac{1}{3}\boldsymbol{I}. \tag{7}$$

At issue here is the Smoluchowski kinetic equation for an imposed simple shear flow, given in Cartesian coordinates (x, y, z) by

$$\boldsymbol{v} = \dot{\gamma}(y, 0, 0), \tag{8}$$

where $\dot{\gamma}$ is the shear rate, assumed constant. The corresponding rate-of-strain $\boldsymbol{D}$ and vorticity tensors $\boldsymbol{\Omega}$ are:

$$\boldsymbol{D} = \frac{1}{2}\dot{\gamma}\begin{pmatrix} 0 & 1 & 0\\ 1 & 0 & 0\\ 0 & 0 & 0\end{pmatrix}, \qquad \boldsymbol{\Omega} = \frac{1}{2}\dot{\gamma}\begin{pmatrix} 0 & 1 & 0\\ -1 & 0 & 0\\ 0 & 0 & 0\end{pmatrix}. \tag{9}$$

We non-dimensionalize the velocity equation (3), (8) and kinetic equation (4) with respect to the relaxation timescale $t_0 = (D_{\mathrm{r}}^0)^{-1}$, which introduces the fundamental flow parameter, the *Peclet number*,

$$Pe = \dot{\gamma}/D_{\mathrm{r}}^0.$$

3. Important expansions

We employ spherical harmonic expansions [27,28] with the basis $Y_l^m(\theta, \phi)$, defined by

$$Y_l^m(\theta, \phi) = P_l^m(\cos\theta)\mathrm{e}^{im\phi}, \tag{10}$$

where $P_l^m(\cos\theta)$ are normalized Legendre polynomials. We now develop expansion formulas for the various terms in the Smoluchowski equation (4), which we will then combine to derive the weak shear construction of f.

From (8), x is the flow direction, y is the direction of the velocity gradient, and z is the vorticity direction. Because of the even parity of the distribution function f, that is, $f(-\boldsymbol{m}) = f(\boldsymbol{m})$, only those spherical harmonics Y_l^m with even l are considered.

3.1. Maier–Saupe potential

For any integrable function $g = g(\boldsymbol{m})$ on the unit sphere $\|\boldsymbol{m}\| = 1$, define T_g as

$$T_g = \boldsymbol{mm} : \langle \boldsymbol{mm} \rangle_g \tag{11}$$

with

$$\langle \boldsymbol{mm} \rangle_g = \int_{\|\boldsymbol{m}\|=1} \boldsymbol{mm} g(\boldsymbol{m}) \, \mathrm{d}\boldsymbol{m}. \tag{12}$$

Since $\boldsymbol{mm}$ is in the span of the first six spherical harmonics, by orthogonality

$$\langle \boldsymbol{mm} \rangle_{Y_l^m} = 0, \quad \text{for } l > 2.$$

Therefore, after some calculation, one can write T_g as an expansion with only six terms:

$$T_g = \frac{4\pi}{3} \langle Y_0^0 \rangle_g Y_0^0 + \frac{8\pi}{15} \sum_{m=-2}^{2} (-1)^m \langle Y_2^{-m} \rangle_g Y_2^m. \tag{13}$$

From this expansion, by the orthogonality property of the harmonics,

$$\begin{cases} T_{Y_0^0} = \frac{4}{3}\pi Y_0^0 \\ T_{Y_2^m} = \dfrac{8}{15}\pi Y_2^m, \quad m = -2, -1, 0, 1, 2, \\ T_{Y_l^m} = 0, \qquad \text{otherwise.} \end{cases} \tag{14}$$

We note that T_g is a linear function of g.

The Maier–Saupe potential for the distribution function f is then given by

$$V_{\mathrm{MS}} = -\frac{3}{2} kTN \boldsymbol{mm} : \langle \boldsymbol{mm} \rangle = -\frac{3}{2} kTN \left(\frac{4\pi}{3} \langle Y_0^0 \rangle_f Y_0^0 + \frac{8\pi}{15} \sum_{m=-2}^{2} (-1)^m \langle Y_2^{-m} \rangle_f Y_2^m \right). \tag{15}$$

3.2. Shear flow

The last term in (4) is the shear flow contribution, which can be written as

$$\begin{aligned} \mathcal{R} \cdot [\boldsymbol{m} \times \dot{\boldsymbol{m}} f] &= \frac{1}{2} Pe \left[(-1 + a \cos 2\phi) \frac{\partial f}{\partial \phi} + \frac{1}{2} a \sin 2\theta \sin 2\phi \, \frac{\partial f}{\partial \theta} \right] - \frac{3}{2} aPe \, (\sin^2 \theta \sin 2\phi) f \\ &= \frac{1}{2} PeG(f), \end{aligned} \tag{16}$$

where the linear function $G(f)$ can be expressed as

$$\begin{aligned} G(f) = a\sqrt{\frac{8\pi}{15}} &\left(\frac{1}{2}(Y_2^1 - Y_2^{-1}) \mathcal{R}_x f + \frac{1}{2} i (Y_2^1 + Y_2^{-1}) \mathcal{R}_y f + (Y_2^2 + Y_2^{-2}) \mathcal{R}_z f \right) \\ &- \mathcal{R}_z f + 3\sqrt{\frac{8\pi}{15}} ia (Y_2^2 - Y_2^{-2}) f. \end{aligned} \tag{17}$$

$\mathcal{R}_x$, $\mathcal{R}_y$ and $\mathcal{R}_z$ are three components of the operator $\mathcal{R}$ in Cartesian coordinates. Applied to the spherical harmonics, we have

$$iG(Y_l^m) = mY_l^m + a\left(\sum_{p=-2}^{2}\alpha_{l,m,p}Y_{l+p}^{m-2} - \sum_{p=-2}^{2}\alpha_{l,-m,p}Y_{l+p}^{m+2}\right),$$

where the coefficients are determined by

$$\begin{cases} \alpha_{l,m,-2} = -\dfrac{(l-2)\sqrt{(-3+l+m)(-2+l+m)(-1+l+m)(l+m)}}{2\sqrt{(-3+2l)(1+2l)}(-1+2l)} \\ \alpha_{l,m,0} = -\dfrac{3\sqrt{(1+l-m)(2+l-m)(-1+l+m)(l+m)}}{2(-1+2l)(3+2l)} \\ \alpha_{l,m,2} = \dfrac{(3+l)\sqrt{(1+l-m)(2+l-m)(3+l-m)(4+l-m)}}{2\sqrt{(1+2l)(5+2l)}(3+2l)} \\ \alpha_{l,m,p} = 0, \quad \text{if } p \neq -2, 0, 2. \end{cases} \tag{18}$$

3.3. The Smoluchowski equation for steady states

Steady states of (4) satisfy

$$\mathcal{R}\cdot\mathcal{R}f - \tfrac{3}{2}N\mathcal{R}\cdot(f\mathcal{R}T_f) - \tfrac{1}{2}PeG(f) = 0. \tag{19}$$

Recall the fundamental spectral property of the rotational diffusion operator $\mathcal{R}\cdot\mathcal{R}$,

$$\mathcal{R}\cdot\mathcal{R}Y_l^m = -l(l+1)Y_l^m. \tag{20}$$

4. Approximate steady solutions in weak shear

We expand the orientational distribution function f in the Peclet number Pe:

$$f = \frac{1}{\sqrt{4\pi}}(f_0 + Pef_1 + Pe^2 f_2 + Pe^3 f_3 + \cdots), \tag{21}$$

and the goal is to determine $f_0, f_1, f_2, \cdots$ associated with the isotropic quiescent state. If we insert this expansion into (19), we have

$$\begin{aligned} &\mathcal{R}\cdot\mathcal{R}f - \frac{3}{2}N\mathcal{R}\cdot(f\mathcal{R}T_f) - \frac{1}{2}PeG(f) \\ &\quad = \frac{1}{\sqrt{4\pi}}\left\{\sum_{k=0}Pe^k\mathcal{R}\cdot\mathcal{R}f_k - \frac{3N}{4\sqrt{\pi}}\sum_{k_1=0}\sum_{k_2=0}Pe^{k_1+k_2}\mathcal{R}\cdot(f_{k_1}\mathcal{R}T_{f_{k_2}}) - \frac{1}{2}Pe\sum_{k=0}Pe^k G(f_k)\right\}. \end{aligned} \tag{22}$$

4.1. Leading order terms and linearized stability

The terms independent of *Pe* give the quiescent Smoluchowski equation for f_0,

$$\mathcal{R}\cdot\mathcal{R}f_0 - \frac{3N}{4\sqrt{\pi}}\mathcal{R}\cdot(f_0\mathcal{R}T_{f_0}) = 0. \tag{23}$$

With the normalization

$$\int_{\|\boldsymbol{m}\|=1} f\,\mathrm{d}\boldsymbol{m} = 1, \tag{24}$$

the *isotropic state* is

$$f_0 = Y_0^0 = \frac{1}{\sqrt{4\pi}}, \tag{25}$$

which solves (23) for all concentrations N. Two nematic branches (for $N > 4.49$) are computed numerically in [27–29], which Onsager [20] characterized analytically. Several valiant attempts (cf. [3,4,7,10,21]) have been made to characterize the flow-induced stable branch(es) of nematic solutions analytically. Absent thus far of an explicit basis for the linearized Smoluchowski equation about the quiescent nematic branch, we restrict hereafter to the isotropic branch.

The *linearized Smoluchowski equation about this isotropic solution* takes the form

$$\frac{\mathrm{d}f}{\mathrm{d}t} = \mathcal{R}\cdot\mathcal{R}f - \frac{3N}{4\sqrt{\pi}}(\mathcal{R}\cdot(f_0\mathcal{R}T_f) + \mathcal{R}\cdot(f\mathcal{R}T_{f_0})) = \mathcal{R}\cdot\mathcal{R}f - \frac{3N}{8\pi}\mathcal{R}\cdot\mathcal{R}T_f. \tag{26}$$

By formulas (14) and (20), we deduce *a basis of independent eigenfunctions of this linearized system*. For example,

$$Y_2^k, \quad k = -2,-1,0,1,2 \tag{27}$$

are five eigenfunctions corresponding to the *multiplicity five* eigenvalue $\lambda_1 = -6(1-(N/5))$;

$$Y_4^k, \quad k = -4,-3,\cdots,3,4 \tag{28}$$

are nine eigenfunctions corresponding to the multiplicity nine eigenvalue $\lambda_2 = -20$;

$$Y_6^k, \quad k = -6,-5,\cdots,5,6 \tag{29}$$

are 13 eigenfunctions corresponding to multiplicity thirteen eigenvalue $\lambda_3 = -42$; and in general, we have the eigenfunctions of

$$Y_{2l}^k, \quad k = -2l,\cdots,2l, \tag{30}$$

corresponding to the eigenvalues $\lambda_l = -2l(2l+1)$, $l = 2,3,\cdots,\infty$. This "block diagonal structure" of the linearized Doi equation is the key to analysis of the isotropic transition in weak flows (cf. See et al. [23] and our discussion below). From this observation, one immediately deduces isotropic solutions are: *asymptotically stable if* $N < 5$, and *unstable for* $N > 5$. The isotropic transition at $N = 5$ is associated with a multiplicity five neutral eigenvalue ($\lambda_1 = 0$). This observation explains why the isotropic instability transition in weak shear is likely to produce a singular expansion for the bifurcation curve, $N - 5 = \mathrm{O}(Pe^{\alpha})$, for some exponent α to be determined. Indeed, See et al. [23] posited $\alpha = 1/2$ and demonstrated self-consistency of an expansion for f in the asymptotic parameter $Pe^{1/2}$. We return to this issue below.

4.2. First order solvability analysis

The terms of order *Pe* determine a non-homogeneous equation for f_1:

$$\mathcal{R}\cdot\mathcal{R}f_1 - \frac{3N}{4\sqrt{\pi}}(\mathcal{R}\cdot(f_0\mathcal{R}T_{f_1}) + \mathcal{R}\cdot(f_1\mathcal{R}T_{f_0})) - \frac{1}{2}G(f_0) = 0. \tag{31}$$

Since

$$T_{f_0} = T_{Y_0^0} = \tfrac{4}{3}\pi Y_0^0, \tag{32}$$

which is constant so that $\mathcal{R}T_{f_0} = 0$, and

$$G(f_0) = \sqrt{\frac{6}{5}}ai(Y_2^2 - Y_2^{-2}), \tag{33}$$

(31) reduces to

$$\mathcal{R}\cdot\mathcal{R}f_1 - \frac{3N}{8\pi}\mathcal{R}\cdot\mathcal{R}T_{f_1} - \sqrt{\frac{3}{10}}ai(Y_2^2 - Y_2^{-2}) = 0. \tag{34}$$

The normalization condition (24) together with (25) imply

$$\int_{\|\boldsymbol{m}\|=1} f_1\,\mathrm{d}\boldsymbol{m} = 0. \tag{35}$$

Therefore, the first order correction to the isotropic state is explicitly and uniquely solvable:

$$f_1 = \frac{i}{2}\sqrt{\frac{5}{6}}\frac{a}{N-5}(Y_2^2 - Y_2^{-2}), \tag{36}$$

which is real since Y_2^{-2} is the complex conjugate of Y_2^2.

4.3. Second-order solvability

The second-order terms give

$$\mathcal{R}\cdot\mathcal{R}f_2 - \frac{3N}{4\sqrt{\pi}}[\mathcal{R}\cdot(f_0\mathcal{R}T_{f_2}) + \mathcal{R}\cdot(f_1\mathcal{R}T_{f_1}) + \mathcal{R}\cdot(f_2\mathcal{R}T_{f_0})] - \frac{1}{2}G(f_1) = 0, \tag{37}$$

or equivalently,

$$\mathcal{R}\cdot\mathcal{R}f_2 - \frac{3N}{8\pi}\mathcal{R}\cdot\mathcal{R}T_{f_2} = \frac{3N}{4\sqrt{\pi}}\mathcal{R}\cdot(f_1\mathcal{R}T_{f_1}) + \frac{1}{2}G(f_1). \tag{38}$$

Denote

$$\alpha_1 = \frac{1}{2}\sqrt{\frac{5}{6}}\frac{a}{N-5}, \tag{39}$$

then we have

$$f_1 = i\alpha_1(Y_2^2 - Y_2^{-2}) \tag{40}$$

$$T_{f_1} = i\alpha_1(T_{Y_2^2} - T_{Y_2^{-2}}) = i\tfrac{8}{15}\pi\alpha_1(Y_2^2 - Y_2^{-2}). \tag{41}$$

Now we expand the right hand side of (38) in spherical harmonics. The following formulas are needed:

$$\begin{aligned}(\mathcal{R}f_1)\cdot(\mathcal{R}T_{f_1}) &= -\tfrac{8}{15}\pi\alpha_1^2\mathcal{R}(Y_2^2 - Y_2^{-2})\cdot\mathcal{R}(Y_2^2 - Y_2^{-2})\\ &= \tfrac{16}{105}\sqrt{\pi}\alpha_1^2(21Y_0^0 - 3\sqrt{5}Y_2^0 - 2Y_4^0 + \sqrt{70}(Y_4^4 + Y_4^{-4}))\end{aligned} \tag{42}$$

$$\begin{aligned}f_1(\mathcal{R}\cdot\mathcal{R}T_{f_1}) &= -\tfrac{8}{15}\pi\alpha_1^2(Y_2^2 - Y_2^{-2})\mathcal{R}\cdot\mathcal{R}(Y_2^2 - Y_2^{-2}) = \tfrac{48}{15}\pi\alpha_1^2(Y_2^2 - Y_2^{-2})^2\\ &= \tfrac{8}{35}\sqrt{\pi}\alpha_1^2(-14Y_0^0 + 4\sqrt{5}Y_2^0 - 2Y_4^0 + \sqrt{70}(Y_4^4 + Y_4^{-4})),\end{aligned} \tag{43}$$

which give

$$\begin{aligned}\mathcal{R}\cdot(f_1\mathcal{R}T_{f_1}) &= (\mathcal{R}f_1)\cdot(\mathcal{R}T_{f_1}) + f_1(\mathcal{R}\cdot\mathcal{R}T_{f_1})\\ &= \tfrac{8}{105}\sqrt{\pi}\alpha_1^2(6\sqrt{5}Y_2^0 - 10Y_4^0 + 5\sqrt{70}(Y_4^4 + Y_4^{-4})).\end{aligned} \tag{44}$$

We also expand $G(f_1)$

$$\begin{aligned}G(f_1) &= i\alpha_1(G(Y_2^2) - G(Y_2^{-2}))\\ &= \alpha_1\left[2(Y_2^2 + Y_2^{-2}) - \frac{2}{7}a\left(\sqrt{6}Y_2^0 - \sqrt{\frac{10}{3}}Y_4^0 + 5\sqrt{\frac{7}{3}}(Y_4^4 + Y_4^{-4})\right)\right].\end{aligned} \tag{45}$$

Therefore, the solution to (38) has the form

$$f_2 = f_2^{(1)}(Y_2^0, Y_2^2, Y_2^{-2}) + f_2^{(2)}(Y_4^0, Y_4^4, Y_4^{-4}), \tag{46}$$

where $f_1^{(1)}$ is a linear function of Y_2^0, Y_2^2, Y_2^{-2}, $f_2^{(2)}$ is a linear function about Y_4^0, Y_4^4, Y_4^{-4}. By formula (14), (38) reduces to

$$-6\left(1 - \frac{N}{5}\right)f_2^{(1)} - 20f_2^{(2)} = \frac{3N}{4\sqrt{\pi}}\mathcal{R}\cdot(f_1\mathcal{R}T_{f_1}) + \frac{1}{2}G(f_1). \tag{47}$$

Then from (44) and (45), we finally arrive at the explicit formulas to construct the second-order term f_2 in the expansion (21) of f:

$$f_2^{(1)} = \frac{1}{2}\left(\frac{5}{6}\right)^{3/2}\frac{a}{6(N-5)^2}\left(\frac{5\sqrt{6}}{7}\frac{a}{N-5}Y_2^0 + (Y_2^2 + Y_2^{-2})\right) \tag{48}$$

$$f_2^{(2)} = \frac{\sqrt{5}}{168\sqrt{6}}\frac{a^2}{(N-5)^2}\left(\sqrt{30}Y_4^0 - 5\sqrt{21}(Y_4^4 + Y_4^{-4})\right). \tag{49}$$

We note that any projection onto the second moment of f, that is, any closure approximation, will induce errors in the term $f_2^{(2)}$.

4.4. The isotropic-nematic transition (See et al. [23])

Note from (36) the above regular perturbation expansion is valid except near the instability transition $N = 5$. To make contact with the fundamental analysis of this bifurcation by See et al. [23], we present

two results that link our regular asymptotic expansion with their scaling behavior. First, we recall their method. They seek a singular asymptotic expansion in a neighborhood of $N = 5$, for $0 < Pe \ll 1$, by positing $O(Pe^{1/2})$ as the correct scaling:

$$N = 5 + cPe^{1/2} + O(Pe), \tag{50}$$

$$f = \frac{1}{\sqrt{4\pi}}(f_0 + Pe^{1/2} f_1 + Pef_2 + \cdots). \tag{51}$$

This scaling assumption, that $(N-5)^2 = O(Pe)$, characterizes *turning points*. Indeed, the breakup of the fifth-order degeneracy, Eq. (27), that characterizes the isotropic instability at $N = 5$, is often a pair of turning points, but degree 5 leaves open the possibility for two disconnected continuous branches to form [36,37], or even for "cusp"-like behavior.

At leading order the isotropic state, independent of N, is $f_0 = Y_0^0 = 1/\sqrt{4\pi}$. At order $O(Pe^{1/2})$,

$$\mathcal{R}\cdot\mathcal{R}f_1 - \frac{15}{8\pi}\mathcal{R}\cdot\mathcal{R}T_{f_1} = 0. \tag{52}$$

By (14) and (20), any function f_1 in the sub-space spanned by the first five spherical harmonics, $S^{(5)} = span\{Y_2^k, k = -2, -1, 0, 1, 2\}$, identically satisfies (52). Furthermore, if f_1 satisfies (52), it must lie in $S^{(5)}$. This fact is equivalent to the earlier observation that the multiplicity-five neutral eigenvalue, $\lambda_1 = 0$, has $S^{(5)}$ as its eigenbasis. To construct f_1, we must continue to the next order, $O(Pe)$, and the equation for f_2 is:

$$\mathcal{R}\cdot\mathcal{R}f_2 - \frac{15}{8\pi}\mathcal{R}\cdot\mathcal{R}T_{f_2} - \frac{c}{5}\mathcal{R}\cdot\mathcal{R}f_1 - 2\sqrt{\pi}\mathcal{R}\cdot(f_1\mathcal{R}f_1) - \frac{1}{2}G(f_0) = 0. \tag{53}$$

As noted above, the first two terms vanish on $S^{(5)}$, but then solvability requires the remaining terms must also vanish on $S^{(5)}$:

$$\tfrac{1}{5}c\mathcal{R}\cdot\mathcal{R}f_1 + 2\sqrt{\pi}\mathcal{R}\cdot(f_1\mathcal{R}f_1) + \tfrac{1}{2}G(f_0)|_{S^{(5)}} = 0. \tag{54}$$

This gives us a system of equations for the averages of the five second spherical harmonics with respect to f_1: $\langle Y_2^{-2}\rangle_{f_1}, \langle Y_2^{-1}\rangle_{f_1}, \langle Y_2^0\rangle_{f_1}, \langle Y_2^1\rangle_{f_1}, \langle Y_2^2\rangle_{f_1}$. (We note these averages are equivalent to the second-moment tensor, Eqs. (65)–(70).)

For simplicity, let $x = \langle Y_2^0\rangle_{f_1}$, $y = \Re(\langle Y_2^2\rangle_{f_1})$, $z = \Im(\langle Y_2^2\rangle_{f_1})$, $u = \Re(\langle Y_2^1\rangle_{f_1})$, $v = \Im(\langle Y_2^1\rangle_{f_1})$ (where $\Re$ and $\Im$ represent the real and imaginary part, respectively). Then we derive from (54) the following 5 equations:

$$\begin{aligned}
&14cy - 5\sqrt{5}(\sqrt{6}(v^2-u^2) + 4xy) = 0, \qquad 6(7c - 10\sqrt{5}x)z + (30\sqrt{30}uv - 35\sqrt{\frac{3}{10}}a) = 0,\\
&7cu + 5\sqrt{5}(xu + \sqrt{6}(zv + yu)) = 0, \qquad 7cv + 5\sqrt{5}(xv + \sqrt{6}(zu - yv)) = 0,\\
&7cx + 5\sqrt{5}(x^2 - 2y^2 - 2z^2 + u^2 + v^2) = 0.
\end{aligned} \tag{55}$$

Analysis of these equations shows one must have $u = v = y = 0$, and x, z and c satisfy:

$$6(7c - 10\sqrt{5}x)z - 35\sqrt{\frac{3}{10}}a = 0, \tag{56}$$

$$7cx + 5\sqrt{5}(x^2 - 2z^2) = 0. \tag{57}$$

To close this system, we follow See et al. [23] and append the marginal stability condition (the Jacobian of (56), (57) is singular), which gives

$$500(x^2 + 2z^2) - 49c^2 = 0. \tag{58}$$

These three equations ((56)-(58)) are explicitly solvable for c, x and z. *One solution* yields the bifurcation curve along which the perturbed isotropic state becomes unstable:

$$N = 5 - \frac{5(2^{3/4})\sqrt{|a|}}{(3^{3/8})\sqrt{21 - 7\sqrt{3}}} Pe^{1/2} \approx 5 - 1.869\sqrt{|a|}Pe^{1/2}, \tag{59}$$

as well as the perturbed solution at order $O(Pe^{1/2})$:

$$\langle Y_2^0\rangle_{f_1} = \frac{7(\sqrt{3}-1)\sqrt{|a|}}{2(2^{1/4})(3^{3/8})\sqrt{5(21 - 7\sqrt{3})}} Pe^{1/2} \approx -0.21\sqrt{|a|}Pe^{1/2}, \qquad \langle Y_2^1\rangle_{f_1} = \Re(\langle Y_2^2\rangle_{f_1}) = 0,$$

$$\Im(\langle Y_2^2\rangle_{f_1}) = -\mathrm{sgn}(a)\frac{7\sqrt{|a|}}{2(2^{1/4})(3^{3/8})\sqrt{5(21 - 7\sqrt{3})}} Pe^{1/2} \approx -0.38\,\mathrm{sgn}(a)\sqrt{|a|}Pe^{1/2}. \tag{60}$$

We thereby recover the result in [23] for $a = 1$, equation (59), together with the extension of the scaling behavior to finite aspect ratio rods ($0 < a \leq 1$) or platelets ($-1 \leq a < 0$). This explicit construction is translated below into a precise form of the second-moment orientation tensor.

To check these asymptotic predictions, we solve the Smoluchowski equation numerically using continuation software AUTO [38] to determine the bifurcation curve (59). For $Pe = 1, 2, 5 \times 10^{-4}$, the transition occurs numerically at

$$\frac{N - 5}{Pe^{1/2}} = 1.870, 1.867, 1.860, \tag{61}$$

respectively, which brackets the theoretical result (59).

We further observe there is *another solution* to ((56)–(58)), to the right of $N = 5$, marking the continuation of the unstable isotropic branch in weak shear:

$$N = 5 + \frac{5(2^{3/4})\sqrt{|a|}}{(3^{3/8})\sqrt{21 - 7\sqrt{3}}} Pe^{1/2} \approx 5 + 1.869\sqrt{|a|}Pe^{1/2}. \tag{62}$$

These two bifurcations reveal *a gap around* $N = 5$, of width $O(Pe^{1/2})$, in which the isotropic equilibria fail to persist in weak shear, as confirmed by our numerical simulations [29].

Our second calculation aims to deduce the $O(Pe^{1/2})$ scaling law at the isotropic transition. We assume $N = 5 + m + \mathrm{HOT}$, where m obeys a scaling law $m = c \cdot Pe^{\alpha}$, $\alpha > 0$, with c to be determined by solvability and marginal stability conditions, and HOT indicates high order terms. We also assume

$$f = \frac{1}{\sqrt{4\pi}}(f_0 + f_1 + \mathrm{HOT}), \tag{63}$$

where $f_1 = O(Pe^{\beta})$ lies in $S^{(5)}$ (as in [23]), and α, β are to be determined. Then we project the Smoluchowski equation onto the space $S^{(5)}$ by neglecting all higher order terms. Details are left to the strong

at heart. We arrive at the same linear system (55), with a replaced by aPe, c replaced by m, and we are able to deduce that $m \approx \pm 1.869|a|Pe^{1/2}$ and $\alpha = \beta = 1/2$. Together with the See et al. [23] results, we have now established the quiescent isotropic instability bifurcation splits apart into two opposite facing *turning points*, separated by a gap of $O(Pe^{1/2})$.

5. Alignment properties from the PDF construction

The explicit construction of the PDF through first- and second-order shear-induced corrections,

$$f \approx \frac{1}{\sqrt{4\pi}}(f_0 + Pef_1 + Pe^2 f_2), \tag{64}$$

is now used to infer physical properties of the shear-perturbed isotropic branch. We first note that the construction of f contains only Y_l^m with m *even*. From [35], if f has zero projections onto Y_l^m for all m odd, then f is an *in-plane*solution of the shear-driven Smoluchowski equation. This notion extends to kinetic theory the traditional definition of in-plane Leslie–Ericksen director and mesoscopic orientation tensors, discussed shortly. The terminology "in-plane" means in the shear deformation plane of the flow and flow gradient. We note at this point that through $O(Pe^2)$, we have established *the weak-shear deformation of the isotropic branch persists as a unique steady distribution, aligned in the flow deformation plane*. We now extract more detailed information about the alignment properties of the shear-perturbed isotropic branch.

The traditional measure of orientation is to project f onto the second-moment tensor $\boldsymbol{Q}$ [35]:

$$Q_{xx} = -\frac{2}{3}\sqrt{\frac{\pi}{5}}a_{2,0} + \sqrt{\frac{8\pi}{15}}\Re(a_{2,2}) \tag{65}$$

$$Q_{yy} = -\frac{2}{3}\sqrt{\frac{\pi}{5}}a_{2,0} - \sqrt{\frac{8\pi}{15}}\Re(a_{2,2}) \tag{66}$$

$$Q_{xy} = -\sqrt{\frac{8\pi}{15}}\Im(a_{2,2}) \tag{67}$$

$$Q_{xz} = -\sqrt{\frac{8\pi}{15}}\Re(a_{2,1}) \tag{68}$$

$$Q_{yz} = \sqrt{\frac{8\pi}{15}}\Im(a_{2,1}), \tag{69}$$

where we recall

$$a_l^m = (-1)^m \langle Y_l^{-m} \rangle_f, \tag{70}$$

and $\Re(\cdot)$ and $\Im(\cdot)$ represent the real and the imaginary part, respectively. From the exact expansions through $O(Pe^2)$ we deduce (with α_1 given in (39))

$$\langle Y_2^0 \rangle_f = \frac{1}{\sqrt{4\pi}} \cdot \frac{25\sqrt{6}a\alpha_1}{42(N-5)^2} Pe^2 \tag{71}$$

$$\langle Y_2^1 \rangle_f = 0 \tag{72}$$

$$\langle Y_2^{-2} \rangle_f = \frac{1}{\sqrt{4\pi}} \cdot \alpha_1 Pe \left(\frac{5}{6(N-5)} Pe + i \right), \tag{73}$$

which now gives the explicit second-moment tensor projection of f for N away from 5:

$$\boldsymbol{Q} = \mathbf{0} + Pe \frac{a}{6(5-N)} \begin{pmatrix} 0 & 1 & 0 \\ 1 & 0 & 0 \\ 0 & 0 & 0 \end{pmatrix} - Pe^2 \frac{5a}{36(5-N)^2} \left[-\frac{5a}{7(N-5)} \begin{pmatrix} 1 & 0 & 0 \\ 0 & 1 & 0 \\ 0 & 0 & -2 \end{pmatrix} + \begin{pmatrix} 1 & 0 & 0 \\ 0 & -1 & 0 \\ 0 & 0 & 0 \end{pmatrix} \right]. \tag{74}$$

This explicit construction is remarkably similar to the Doi closure model for $\boldsymbol{Q}$ [19]. We can now explicitly provide the eigenvalues and eigenvectors of $\boldsymbol{Q}$ to determine the mesoscopic alignment properties of the explicit kinetic PDF.

- The eigenvalues of $\boldsymbol{Q}$ through O(Pe) are distinct, in descending order,

$$\lambda_1 = \frac{Pe}{6} \left| \frac{a}{5-N} \right|, \qquad \lambda_2 = 0, \qquad \lambda_3 = -\frac{Pe}{6} \left| \frac{a}{5-N} \right|. \tag{75}$$

We deduce $\boldsymbol{Q}$ is *biaxial*. The *degree of biaxiality*, $0 \le b \le 1$, [16] is defined by

$$b = \sqrt{1 - \frac{6\mathrm{Tr}(\boldsymbol{Q}^3)^2}{\mathrm{Tr}(\boldsymbol{Q}^2)^3}}, \tag{76}$$

which is depicted in Fig. 1(left) versus N using the O(Pe^2) eigenvalue formulas for $Pe = 0.1$. This is one measure of the relative focusing of the distribution function with respect to the three director axes, with $b = 1$ corresponding to maximum biaxiality. Note the distribution remains defocused until N approaches the nematic transition.

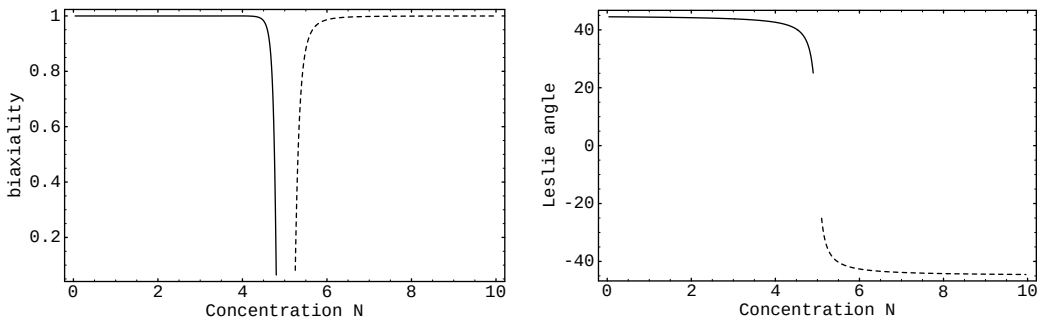

Fig. 1. Left: biaxiality parameter b for $Pe = 0.1$, $a = 1$. Right: scaling behavior of the Leslie angle versus concentration (N) for $Pe = 0.1$ and $a = 1$. The solid line indicates stable solutions, the dashed line corresponds to unstable solutions.

- The intermediate eigenvalue, $\lambda_2 = 0$ through O(Pe), has director $\boldsymbol{n}_2 = (0, 0, 1)$, aligned with the vorticity axis. Thus, the isotropic state can never become "logrolling", with peak orientation orthogonal to the shearing plane. Indeed, *at leading order in Pe, there is no focusing of the distribution function along the vorticity axis*.
- The *major director* $\boldsymbol{n}_1 = (\cos\phi, \sin\phi, 0)$ (associated with the largest degree of order λ_1) *always lies in the shear plane* with $\boldsymbol{n}_3 \perp \boldsymbol{n}_1$ also in-plane. The formulae for λ_i indicate that the LCP molecules break their random orientation by shifting primary alignment completely within the shearing plane.
- The *major director* $\boldsymbol{n}_1$ is parallel to

$$\left(Q_{xx} - Q_{yy} + \sqrt{(Q_{xx} - Q_{yy})^2 + 4Q_{xy}^2}, 2Q_{xy}, 0\right), \tag{77}$$

so that the *Leslie alignment angle ϕ takes the explicit form through* O(Pe^2):

$$\cos 2\phi = \mathrm{sgn}[a(5 - N)]\frac{1}{\lambda_\mathrm{L}}, \tag{78}$$

where

$$\lambda_\mathrm{L} = \sqrt{1 + \left(\frac{6(1 - (N/5))}{Pe}\right)^2} > 1. \tag{79}$$

This expression shows several important features:

- Flow-alignment always occurs for stable ($N < 5$) *and* unstable ($N > 5$) nearly isotropic states, i.e., $\lambda_\mathrm{L} \geq 1$. *Tumbling or other oscillatory responses are impossible for the shear perturbed isotropic branch in the weak flow limit*.
- The mesoscopic Leslie angle through O(Pe^2) is independent of aspect ratio (except the sign of a), equations (78) and (79), depicted versus N in Fig. 1 (right) for fixed $Pe = 0.1$.
- The *stable alignment angle in the weak shear limit, $Pe \to 0$*, is 45° (respectively −45°), *for all rod-like (respectively plate-like) molecular aspect ratios $a > 0$ (respectively $a < 0$), and for all concentrations $N < 5$*. Fig. 2 shows the distribution function f as a function of the polar angle θ (measured with respect to the vorticity axis) and azimuthal angle ϕ (measured in the plane of flow and flow gradient). The molecular and flow parameters chosen are $a = 1$, $N = 2$, $Pe = 0.1$. From Fig. 2, f is not very focused in weak shear. The peak of the distribution is *in-plane*, $\theta = \pi/2$, and the Leslie alignment angle ϕ is slightly below $\pi/4$.
- Fig. 3 shows the Leslie alignment angle versus weak shear $0 < Pe < 0.8$ for several fixed concentrations. It is clearly a decreasing function of Pe with scaling behavior consistent with (78) and (79). As the shear rate increases from zero, the Leslie angle decreases from 45^0 (for rods) toward the flow axis.

- The shear-induced flow birefringence is measured by the differences in eigenvalues of $\boldsymbol{Q}$, which from the O(Pe) formulas for λ_i are:

$$\lambda_1 - \lambda_2 = \left|\frac{a}{5 - N}\right|\frac{Pe}{6}, \qquad \lambda_3 - \lambda_2 = -\left|\frac{a}{5 - N}\right|\frac{Pe}{6}. \tag{80}$$

These are depicted in Fig. 4 versus N for $Pe = 0.1$ using the O(Pe^2) formulas.

The above construction breaks down in an O($Pe^{1/2}$) neighborhood of the critical concentration $N = 5$ where the isotropic state becomes unstable. Our singular analysis shows a *gap* forms, $(5 - 1.869Pe^{1/2}, 5 + 1.869Pe^{1/2})$, where the quiescent isotropic state does not persist. This result confirms mesoscopic second-

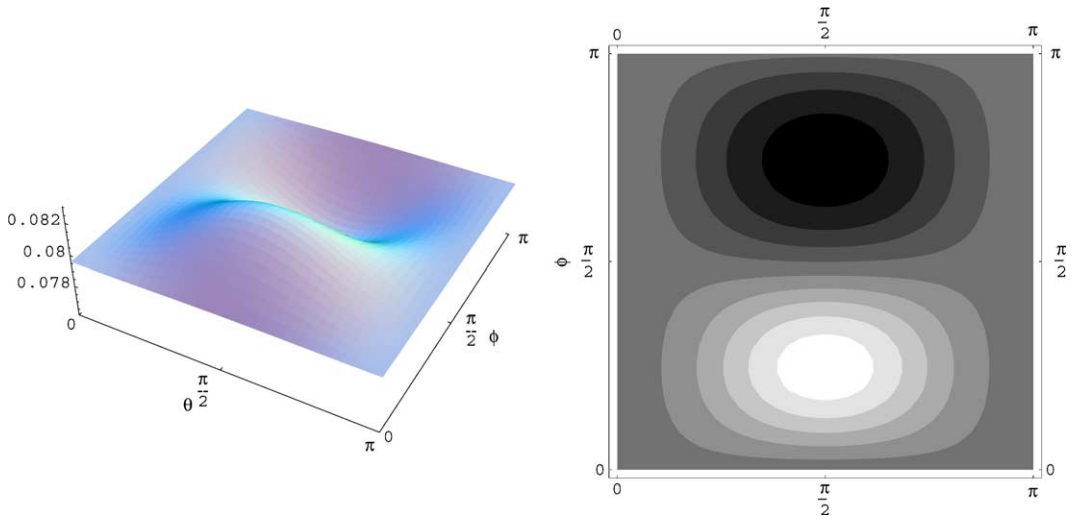

Fig. 2. Left: the distribution function $f(\theta, \phi)$ approximated by second-order expansion. Right: the contour plot of the distribution function $f(\theta, \phi)$. The parameters chosen are: $a = 1$ (infinitely thin rods), $N = 2$, $Pe = 0.1$. The peak of the distribution is at $\theta = \pi/2$ (i.e., in-plane major director) with Leslie alignment angle $\phi \approx \pi/4$.

moment tensor analysis [19] and numerical simulations of both kinetic theory [28,29] and mesoscopic tensor models [13,18]. Based on the singular asymptotics in Section 4.2, we now construct the explicit second-moment tensor projection of f along the isotropic-nematic transition curve:

$$\boldsymbol{Q} = \mathbf{0} + Pe^{1/2} \left\{ \frac{7(\sqrt{3}-1)\sqrt{|a|}}{30(2^{1/4})(3^{3/8})\sqrt{21-7\sqrt{3}}} \begin{pmatrix} 1 & 0 & 0 \\ 0 & 1 & 0 \\ 0 & 0 & -2 \end{pmatrix} + \operatorname{sgn}(a) \frac{7\sqrt{|a|}}{5(2^{3/4})(3^{5/8})\sqrt{21-7\sqrt{3}}} \begin{pmatrix} 0 & 1 & 0 \\ 1 & 0 & 0 \\ 0 & 0 & 0 \end{pmatrix} \right\}. \tag{81}$$

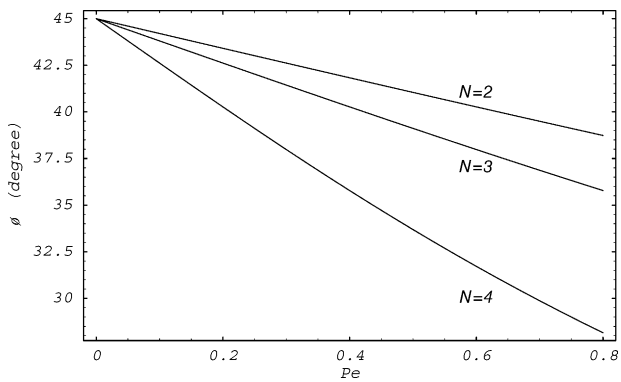

Fig. 3. Scaling behavior of the Leslie alignment angle versus normalized shear rate (*Pe*) and concentration (*N*).

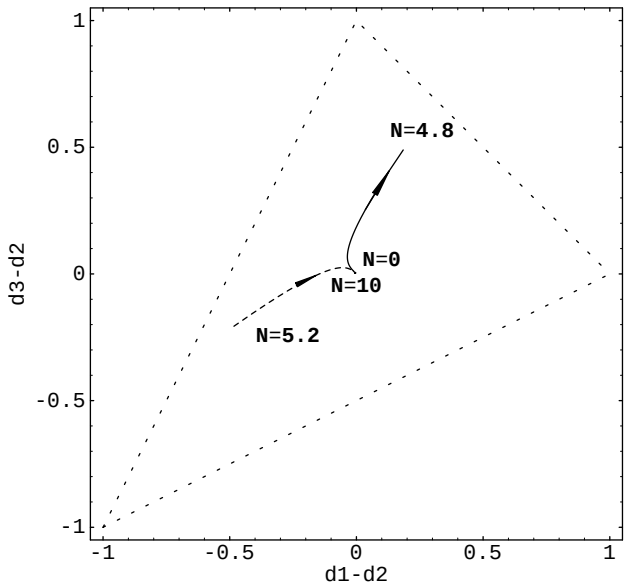

Fig. 4. Order parameters for $Pe = 0.1$ and $a = 1$. The solid curve ($0 \le N \le 4.8$) is the stable flow-aligning branch, while the dashed curve is the unstable flow-aligning branch. The isotropic state ($d_1 = d_2 = d_3 = 1/3$) lies at the center ($N = 0$) and then biaxial states emerge as N increases toward 4.8.

The eigenvalues of this tensor are

$$\lambda_1 = 0.17\sqrt{|a|Pe}, \qquad \lambda_2 = -0.06\sqrt{|a|Pe}, \qquad \lambda_3 = -0.11\sqrt{|a|Pe}. \tag{82}$$

Therefore, $\boldsymbol{Q}$ is biaxial. The shear-induced flow birefringence is given by

$$\lambda_1 - \lambda_3 = 0.28\sqrt{|a|Pe}, \qquad \lambda_2 - \lambda_3 = 0.05\sqrt{|a|Pe}. \tag{83}$$

Comparison of (74) and (81) reveals a "jump" in the scaling behavior and in the Q tensor components as one passes through the bifurcation curve.

6. Rheological properties

The extra stress in dimensional form is given by [5]

$$\begin{aligned}\tau = {} & (2\eta + 3\nu kT\zeta_3(a))\boldsymbol{D} + 3a\nu kT[\boldsymbol{Q} - N(\boldsymbol{Q} + \tfrac{1}{3}\boldsymbol{I})\boldsymbol{Q} + N\boldsymbol{Q} : \langle \boldsymbol{mmmm}\rangle] \\ & + 3\nu kT[\zeta_1(a)(\boldsymbol{DM} + \boldsymbol{MD}) + \zeta_2(a)\boldsymbol{D} : \langle \boldsymbol{mmmm}\rangle],\end{aligned} \tag{84}$$

where

$$\begin{aligned}&\zeta_3 = \frac{\zeta^{(0)}}{I_1}, \qquad \zeta_1 = \zeta^{(0)}\left(\frac{1}{I_3} - \frac{1}{I_1}\right), \qquad \zeta_2 = \zeta^{(0)}\left[\frac{J_1}{I_1 J_3} + \frac{1}{I_1} - \frac{2}{I_3}\right], \qquad r = \sqrt{\frac{1+a}{1-a}}, \\ &I_1 = 2r\int_0^\infty \frac{dx}{\sqrt{(r^2+x)}(1+x)^3}, \qquad I_3 = r(r^2+1)\int_0^\infty \frac{dx}{\sqrt{(r^2+x)}(1+x)^2(r^2+x)}, \\ &J_1 = r\int_0^\infty \frac{xdx}{\sqrt{(r^2+x)}(1+x)^3}, \qquad J_3 = r\int_0^\infty \frac{xdx}{\sqrt{(r^2+x)}(1+x)^2(r^2+x)},\end{aligned} \tag{85}$$

where ν is the number density of LCP molecules per unit volume, and $\zeta^{(0)}$ is a free parameter depending on a that must be experimentally fitted. In the calculations below, because we do not know the exact dependence of ζ_0 on a, we choose constant $\zeta^{(0)} = 0.01$. For rod-like polymers $r = 10$ ($a \approx 0.98$), from (85), the values of these parameters are computed: $\zeta_1 \approx 0.0004$, $\zeta_2 \approx 0.15$, $\zeta_3 \approx 0.01$. For discotic polymers $r = \frac{1}{10}$ ($a \approx -0.98$), $\zeta_1 \approx -0.044$, $\zeta_2 \approx 0.053$, $\zeta_3 \approx 0.05$. We neglect the isotropic viscosity, i.e., $\eta = 0$, and non-dimensionalize by a characteristic entropic stress $\tau_0 = 3\nu kT$.

The second-moment tensor $\boldsymbol{Q}$ has been explicitly constructed in (74). To compute the stress tensor τ, we also need to construct the fourth-moment tensor $\langle \boldsymbol{mmmm} \rangle$. They are explicitly given in the Appendix A.

The steady shear stress σ and the first and second normal stress differences N_1, N_2 in dimensionless form are defined by

$$N_1 = \tau_{xx} - \tau_{yy},$$

$$N_2 = \tau_{yy} - \tau_{zz},$$

$$\sigma = \tau_{xy}/Pe.$$

Through $O(Pe^2)$, explicit expansions for these rheological properties follow from our analysis:

$$N_1 = \frac{1}{18(5-N)} a^2 Pe^2 + O(Pe^4), \tag{86}$$

$$N_2 = \frac{3a^2 - 7a + 42\zeta_1 + 12\zeta_2}{252(5-N)} aPe^2 + O(Pe^4), \tag{87}$$

$$\sigma = \frac{1}{30}(a^2 + 10\zeta_1 + 2\zeta_2 + 15\zeta_3) + \frac{1}{Re} + O(Pe)^2. \tag{89}$$

Presuming the isotropic viscosity is negligible ($1/Re = 0$), these features are plotted in Fig. 5 for a rod-like aspect ratio $r = 10$ and Fig. 6 for a plate-like aspect ratio $r = 1/10$. The essential results are:

- Both N_1 and N_2 are of order $O(Pe^2)$ for N sufficiently dilute, and therefore, nearly zero in weak shear.
- $N_1 > 0$ and $N_2 < 0$ at stable dilute concentrations, $0 < N < 5 - \delta$, with $\delta = O(Pe^{1/2})$.
- As N approaches 5, N_1 and N_2 grow in magnitude, but the asymptotic expansions break down in this limit. These properties of N_1 and N_2 confirm mesoscopic predictions [19].
- The scaled apparent viscosity σ is independent of concentration N at $O(Pe)$, then exhibits "concentration thinning" for both rods and discotics, as the concentration increases towards the nematic transition.

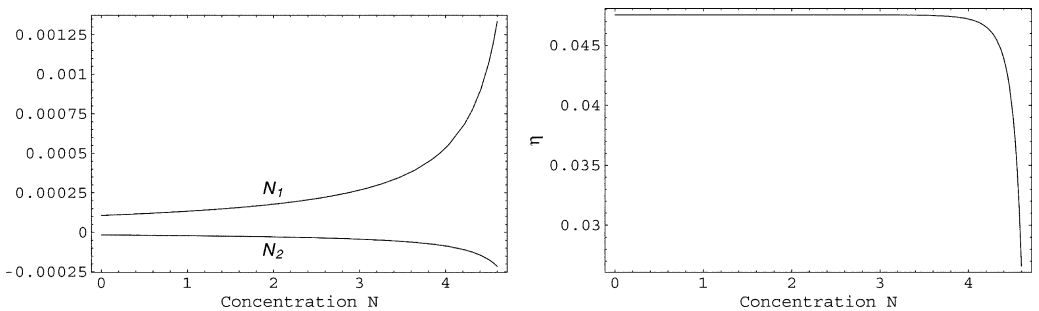

Fig. 5. Scaled normal stress differences N_1, N_2, and apparent viscosity η for rod-like polymers $r = 10$ at $Pe = 0.1$.

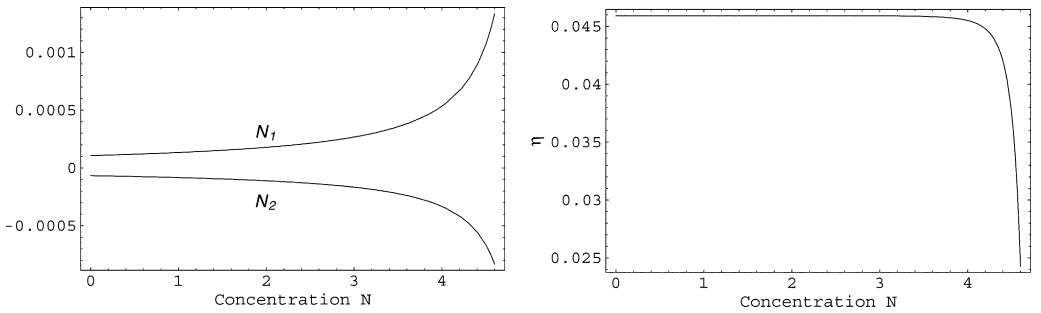

Fig. 6. Scaled normal stress differences N_1, N_2, and apparent viscosity η for plate-like polymers $r = 1/10$ at $Pe = 0.1$.

We are unaware of experimental data to benchmark these predictions. However, they are consistent with numerical simulations of the full kinetic equation for infinite aspect ratio rods [29]. We note the normal stress differences N_1 and N_2 qualitatively confirm the mesoscopic predictions in [19]. The shear stress σ confirms mesoscopic behavior except near the instability transition, where the "thinning" or "thickening" of σ is sensitive to closure approximations [19].

7. Conclusion

The goals outlined in the abstract and introduction have been met. An explicit construction and stability analysis of the PDF of Doi kinetic theory in the dilute concentration and weak flow regime have been provided. The formulas are confirmed by direct numerical simulations, and then used to infer experimental data for the primary alignment of the PDF, the relative focusing of the distribution, and stress measurements. Most importantly, these constructions provide rigorous scaling behavior of flow-aligned steady orientational distributions in weak shear with respect to molecular and flow parameters. Our results are complementary to the analysis of See et al. [23], who determined the scaling behavior of the isotropic instability transition in weak flow. Together, our analyses covers the weak flow perturbation properties of the isotropic state for all concentrations.

Acknowledgements

Effort sponsored by the Air Force Office of Scientific Research, Air Force Materials Command, USAF, under grant no. F49620-02-1-0086, and the National Science Foundation through grants DMI-0115445, DMS-0204243 and DMS-0308019. This work is supported in part by the NASA University Research, Engineering and Technology Institute on Bio Inspired Materials (BIMat) under award no. NCC-1-02037.

Appendix A

Suppose $f(\boldsymbol{m})$ has the spheric harmonic expansion

$$f(\boldsymbol{m}) = \sum_{l=0}^{\infty} \sum_{m=-l}^{l} a_{lm} Y_l^m(\theta, \phi). \tag{A.1}$$

Denote by $\mathcal{M}$ the fourth-moment tensor $\langle \boldsymbol{mmmm} \rangle$. Components of $\mathcal{M}$ can be computed as (nine of them are independent):

$$\mathcal{M}_{1111} = \tfrac{1}{105}\sqrt{\pi}\left(42a_{00} - 12\sqrt{5}a_{20} + 12\sqrt{30}\Re(a_{22}) + 6a_{40} - 4\sqrt{10}\Re(a_{42}) + 2\sqrt{70}\Re(a_{44})\right)$$

$$\mathcal{M}_{1112} = \frac{2}{21}\sqrt{\frac{2\pi}{5}}\left(-3\sqrt{3}\Im(a_{22}) + \Im(a_{42}) - \sqrt{7}\Im(a_{44})\right)$$

$$\mathcal{M}_{1113} = -\frac{2}{21}\sqrt{\frac{\pi}{5}}\left(3\sqrt{6}\Re(a_{21}) - 3\Re(a_{41}) + \sqrt{7}\Re(a_{43})\right)$$

$$\mathcal{M}_{1122} = \tfrac{1}{105}\sqrt{\pi}\left(14a_{00} + 2a_{40} - 4\sqrt{5}a_{20} - 2\sqrt{70}\Re(a_{44})\right)$$

$$\mathcal{M}_{1123} = \frac{2}{21}\sqrt{\frac{\pi}{5}}\left(\sqrt{6}\Im(a_{21}) - \Im(a_{41}) + \sqrt{7}\Im(a_{43})\right)$$

$$\mathcal{M}_{1133} = \tfrac{1}{105}\sqrt{\pi}\left(14a_{00} + 2\sqrt{5}a_{20} - 8a_{40} + 2\sqrt{30}\Re(a_{22}) + 4\sqrt{10}\Re(a_{42})\right)$$

$$\mathcal{M}_{1222} = \frac{2}{21}\sqrt{\frac{2\pi}{5}}\left(-3\sqrt{3}\Im(a_{22}) + \Im(a_{42}) + \sqrt{7}\Im(a_{44})\right)$$

$$\mathcal{M}_{1223} = \frac{2}{21}\sqrt{\frac{\pi}{5}}\left(-\sqrt{6}\Re(a_{21}) + \Re(a_{41}) + \sqrt{7}\Re(a_{43})\right)$$

$$\mathcal{M}_{1233} = -\frac{2}{21}\sqrt{\frac{2\pi}{5}}\left(\sqrt{3}\Im(a_{22}) + 2\Im(a_{42})\right)$$

$$\mathcal{M}_{1333} = -\frac{2}{21}\sqrt{\frac{\pi}{5}}\left(3\sqrt{6}\Re(a_{21}) + 4\Re(a_{41})\right)$$

$$\mathcal{M}_{2222} = \tfrac{1}{105}\sqrt{\pi}\left(42a_{00} - 12\sqrt{5}a_{20} - 12\sqrt{30}\Re(a_{22}) + 6a_{40} + 4\sqrt{10}\Re(a_{42}) + 2\sqrt{70}\Re(a_{44})\right)$$

$$\mathcal{M}_{2223} = -\frac{2}{21}\sqrt{\frac{\pi}{5}}\left(-3\sqrt{6}\Im(a_{21}) + 3\Im(a_{41}) + \sqrt{7}\Im(a_{43})\right)$$

$$\mathcal{M}_{2233} = \frac{\sqrt{\pi}}{105}\left(14a_{00} + 2\sqrt{5}a_{20} - 8a_{40} - 2\sqrt{30}\Re(a_{22}) - 4\sqrt{10}\Re(a_{42})\right)$$

$$\mathcal{M}_{2333} = \frac{2}{21}\sqrt{\frac{\pi}{5}}\left(3\sqrt{6}\Im(a_{21}) + 4\Im(a_{41})\right)$$

$$\mathcal{M}_{3333} = \frac{\sqrt{\pi}}{105}\left(42a_{00} + 16a_{40} + 24\sqrt{5}a_{20}\right).$$

References

[1] J.L. Ericksen, Anisotropic fluids, Arch. Rational Mech. Anal. 4 (1960) 231–237.
[2] F.M. Leslie, Some constitutive equations for liquid crystals, Arch. Rational Mech. Anal. 28 (1968) 265–283.
[3] N. Kuzuu, M.J. Doi, Constitutive equation for nematic liquid crystals under weak velocity gradient derived from a molecular kinetic equation, Phys. Soc. Jpn. 52 (1983) 3486–3494.
[4] N. Kuzuu, M.J. Doi, Constitutive equation for nematic liquid crystals under weak velocity gradient derived from a molecular kinetic equation. II. Leslie coefficients for rodlike polymers, Phys. Soc. Jpn. 53 (1984) 1031–1040.
[5] Q. Wang, A hydrodynamic theory for solutions of nonhomogeneous nematic liquid crystalline polymers of different configuration, J. Chem. Phys. 116 (20) (2002) 9120–9136.
[6] Q. Wang, M.G. Forest, R. Zhou, A hydrodynamic theory for solutions of nonhomogeneous nematic liquid crystalline polymers with density variations, in: Proceedings of ASME International Mechanical Engineering Congress, IMECE2002-32189, N.O., LA, 17–22 November 2002.
[7] L.A. Archer, R.G. Larson, A molecular theory of flow alignment and tumbling in sheared nematic liquid crystals, J. Chem. Phys. 103 (1995) 3108–3111.
[8] P.G. de Gennes, J. Prost, The Physics of Liquid Crystals, Oxford University Press, Oxford, 1993.
[9] A.N. Beris, B.J. Edwards, Thermodynamics of Flowing Systems with Internal Microstructure, Oxford Science Publications, Oxford, 1994.
[10] M. Kroger, H.S. Sellers, Viscosity coefficients for anisotropic, nematic fluids based on structural theories of suspensions, J. Chem. Phys. 103 (1995) 807–817.
[11] R.G. Larson, The Structure and Rheology of Complex Fluids, Oxford University Press, Oxford, 1998.
[12] F. Cocchini, C. Aratari, G. Marrucci, Tumbling of rodlike polymers in the liquid-crystalline phase under shear flow, Macromolecules 23 (1990) 4446–4451.
[13] A.V. Bhave, R.K. Menon, R.C. Armstrong, R.A. Brown, A constitutive equation for liquid crystalline polymer solutions, J. Rheol. 37 (1993) 413–441.
[14] Y. Farhoudi, A.D. Rey, Shear flows of nematic polymers. I. Orienting modes, bifurcations, and steady state rheological predictions, J. Rheol. 37 (2) (1993) 289–314.
[15] Q. Wang, Biaxial steady states and their stability in shear flows of liquid crystal polymers, J. Rheol. 41 (5) (1997) 943–970.
[16] G. Rienacker, S. Hess, Orientational dynamics of nematic liquid crystals under shear flow, Phys. A 267 (1999) 294–321.
[17] P.L. Maffettone, A.M. Sonnet, E.G. Virga, Shear-induced biaxiality in nematic polymers, J. Non-Newtonian Fluid Mech. 90 (2000) 283–297.
[18] M.G. Forest, Q. Wang, Monodomain response of finite-aspect-ratio macromolecules in shear and related linear flows, Rheol. Acta 42 (2003) 20–46.
[19] M.G. Forest, R. Zhou, Q. Wang, Full-tensor alignment criteria for sheared nematic polymers, J. Rheol. 47 (1) (2003) 105–127.
[20] L. Onsager, The effects of shape on the interaction of colloidal particles, Ann. N.Y. Acad. Sci. 51 (1949) 627–659.
[21] A.N. Semenov, Rheological properties of a liquid crystal solution of rod-like molecules, Sov. Phys. JETP 66 (1983) 321.
[22] G. Marrucci, P.L. Maffettone, Description for the liquid crystalline phase of rodlike polymers at high shear rates, Macromolecules 22 (1989) 4076–4082.
[23] H. See, M. Doi, R.G. Larson, The effect of steady flow fields on the isotropic-nematic phase transition of rigid rod-like polymers, J. Chem. Phys. 92 (1) (1990) 792–800.
[24] P.T. Mather, D.S. Pearson, R.G. Larson, Flow patterns and disclination-density measurements in sheared nematic liquid crystals. I. Flow-aligning 5CB, Liq. Cryst. 20 (5) (1996) 527–538.
[25] P.T. Mather, D.S. Pearson, R.G. Larson, Flow patterns and disclination-density measurements in sheared nematic liquid crystals. II. Tumbling 8CB, Liq. Cryst. 20 (5) (1996) 539–546.
[26] P. Constantin, I. Kevrekidis, E.S. Titi, Asymptotic states of a Smoluchowski equation, 2003, in press.
[27] R.G. Larson, H. Ottinger, The effect of molecular elasticity on out-of-plane orientations in shearing flows of liquid crystalline polymers, Macromolecules 24 (1991) 6270–6282.
[28] V. Faraoni, M. Grosso, S. Crescitelli, P.L. Maffettone, The rigid-rod model for nematic polymers: an analysis of the shear flow problem, J. Rheol. 43 (1999) 829–843.
[29] M.G. Forest, Q. Wang, R. Zhou, The weak shear phase diagram for nematic polymers, Rheol. Acta, 2003, in press.
[30] G. Marrucci, F. Greco, Flow behavior of liquid crystalline polymers, Adv. Chem. Phys. 86 (1993) 331–404.

[31] V.I. Stepanov, Statistical and Dynamical Problems of the Elasticity and Viscoelasticity, Urals Branch of the USSR Academy of Science, Sverdlovsk (in Russian).
[32] T. Tsuji, A. Rey, Effect of long range order on sheared liquid crystalline polymers. Part 1. Compatibility between tumbling behavior and fixed anchoring, J. Non-Newtonian Fluid Mech. 73 (1997) 127–152.
[33] J. Feng, G. Sgalari, G. Leal, A theory for flowing nematic polymers with orientational distortions, J. Rheol. 44 (5) (2000) 1085–1101.
[34] M. Grosso, R. Keunings, S. Crescitelli, P.L. Maffettone, Prediction of chaotic dynamics in sheared liquid crystalline polymers, Phys. Rev. Lett. 86 (14) (2001) 3184–3187.
[35] M.G. Forest, R. Zhou, Q. Wang, Symmetries of the Doi kinetic theory for nematic polymers of arbitrary aspect ratio: at rest and in linear flows, Phys. Rev. E 66 (3) (2002) 031712.
[36] M.G. Forest, Q. Wang, H. Zhou, Homogeneous pattern selection and director instabilities of nematic liquid crystal polymers induced by elongational flows, Phys. Fluids 12 (3) (2000) 490–498.
[37] M.G. Forest, Q. Wang, H. Zhou, On the flow-phase diagram for discotic liquid crystals in uniaxial extension and compression, Liq. Cryst. 28 (5) (2001) 717–720.
[38] E.J. Doedel, et al., AUTO97: continuation and bifurcation software for ordinary differential equations, Concordia University, 1997.